9180 *Inorg. Chem.* **2009**, *48*, 9180–9184
DOI: 10.1021/ic900854x

Inorganic Chemistry
Article

Morphology-Controlled Synthesis of Barium Titanate Nanostructures

Kuan-Chih Huang,[†] Tung-Ching Huang,[†] and Wen-Feng Hsieh*[,‡]

[†]*Department of Photonics and Institute of Electro-Optical Engineering, National Chiao Tung University, 1001 Tahsueh Rd., Hsinchu, Taiwan, and* [‡]*Institute of Electro-Optical Science and Engineering, National Cheng Kung University, 1 Dahsueh Rd., Tainan, Taiwan*

Received May 3, 2009

This study reports the synthesis of morphology-controlled $BaTiO_3$ nanostructures such as spherical, cube-shaped and rod-shaped $BaTiO_3$ using a molten-salt synthesis method. This method synthesized products from a reaction of BaO/$BaCO_3$ and TiO_2 with a eutectic mixture of NaCl-KCl flux at 700 °C for 1 h. The experiment used powder X-ray diffraction, field emission scanning electron microscopy, and transmission electron microscopy to investigate the structure and morphology of the products. Moreover, the current work also provides a proposed synthetic mechanism of $BaTiO_3$ in the molten salt to illustrate the *in situ* transformation mechanism of $BaTiO_3$ nanostructures in the reaction. The results of the study revealed that the initial shape of the titania and the dissolution rate of the initial precursors critically determine the shapes of the final products.

I. Introduction

Over the past decade, ferroelectric nanomaterials have attracted much attention because of their potential applications.[1−3] Among various ferroelectric ternary transition-metal oxides, $BaTiO_3$ is one of the best materials, possessing a perovskite structure with the Curie temperature of about 132 °C, and has drawn major interest for ferroelectric applications. It exhibits a large nonlinear optical coefficient and a large dielectric constant found in widespread applications in the manufacture of multilayer capacitors, thermistors, electro-optical devices, transducers, high-k dielectrics, dynamic random-access memory, and field effect transistors.[4−6] Recently, much effort has been given to morphology-controlled synthesis of crystalline ferroelectric oxide materials because the effects of a large nonlinear optical coefficient and a large dielectric constant are highly dependent on the size and shape.[7] Of various nanostructures, low-dimensional nanostructures, such as nanoparticles, nanowires, nanocubes, and nanorods, have especially received great interest from the scientific and engineering communities[8,9] because these structures exhibit distinct physical and chemical properties from bulk materials because of their smaller particle sizes and larger surface-to-volume ratios. Thus, many studies have probed the optical,[10] electronic,[11] and magnetic[12] properties of these nanostructures.

Scientists expect one-dimensional (1D) structures, nanorods, and nanowires to provide new alternatives for developing devices because of recent theoretical studies from first principles and experiments on ferroelectric nanowires. This possibility primarily arises because the size-dependent ferroelectricity of 1D structures functions with much smaller diameters than do 0-D structures (nanoparticle), and the Curie temperature is reduced as the diameter of the 1D structure is reduced.[13−15] Wang et al.[16] also reported a method for researching the axial poling and switching in 1D $BaTiO_3$ nanowires by using piezoresponse force microscopy (PFM).

So far, many methods exist for synthesizing $BaTiO_3$ 1D structures. The major methods can be approximately separated into two groups. The first and the earliest process is molten-salt synthesis; the second process is a hydrothermal

*To whom correspondence should be addressed. E-mail: wfhsieh@mail.nctu.edu.tw. Phone: 886-3-5712121, ext.56316.

(1) Auciello, O.; Scott, J. F.; Ramesh, R. *Phys. Today* **1998**, *51*, 22.
(2) Scott, J. F. In *Ferroelectric memories today*; Prague, Czech Republic, Jul 12−16, 1999; Gordon Breach Sci Publ Ltd: Prague, Czech Republic, 1999; p 247.
(3) Ahn, C. H.; Rabe, K. M.; Triscone, J. M. *Science* **2004**, *303*, 488.
(4) Phule, P. P.; Risbud, S. H. *J. Mater. Sci.* **1990**, *25*, 1169.
(5) Kishi, H.; Mizuno, Y.; Chazono, H. *Jpn. J. Appl. Phys.* **2003**, *42*, 1.
(6) Scott, J. F. *Science* **2007**, *315*, 954.
(7) O'Brien, S.; Brus, L.; Murray, C. B. *J. Am. Chem. Soc.* **2001**, *123*, 12085.
(8) Alivisatos, A. P. *Science* **1996**, *271*, 933.
(9) Hu, J. T.; Odom, T. W.; Lieber, C. M. *Acc. Chem. Res.* **1999**, *32*, 435.
(10) Huang, M. H.; Mao, S.; Feick, H.; Yan, H. Q.; Wu, Y. Y.; Kind, H.; Weber, E.; Russo, R.; Yang, P. D. *Science* **2001**, *292*, 1897.
(11) Thurn-Albrecht, T.; Schotter, J.; Kastle, C. A.; Emley, N.; Shibauchi, T.; Krusin-Elbaum, L.; Guarini, K.; Black, C. T.; Tuominen, M. T.; Russell, T. P. *Science* **2000**, *290*, 2126.
(12) Liang, W. J.; Bockrath, M.; Bozovic, D.; Hafner, J. H.; Tinkham, M.; Park, H. *Nature* **2001**, *411*, 665.
(13) Geneste, G.; Bousquet, E.; Junquera, J.; Ghosez, P. *Appl. Phys. Lett.* **2006**, *88*, 3.
(14) Hong, J. W.; Fang, D. N. *Appl. Phys. Lett.* **2008**, *92*, 3.
(15) Spanier, J. E.; Kolpak, A. M.; Urban, J. J.; Grinberg, I.; Lian, O. Y.; Yun, W. S.; Rappe, A. M.; Park, H. *Nano Lett.* **2006**, *6*, 735.
(16) Wang, Z. Y.; Suryavanshi, A. P.; Yu, M. F. *Appl. Phys. Lett.* **2006**, *89*, 3.

 Published on Web 09/01/2009

process with or without a template.[17−22] In the first group, Hayashi et al.[23] reported the synthesis of rod-shaped $BaTiO_3$ powder particles by rod-shaped $TiO_2 \cdot nH_2O$ and $BaCO_3$ in the molten chloride. Mao et al.[24] produced single-crystalline $BaTiO_3$ nanorods and $SrTiO_3$ nanoparticles by using a large-scale and facile solid-state reaction with nonionic surfactant. Recently, Deng et al.[25] obtained the $BaTiO_3$ 1D nanostructure by using a surfactant-free approach in a nonaqueous molten salt media. Because the $BaTiO_3$ 1D nanostructure is difficult to obtain because of the isotropy of the $BaTiO_3$ tetragonal crystal structure and the anisotropy of the 1D structure, the control of nucleation and growth of 1D nanostructure materials is still a big challenge.[26] Because of these limitations, we believe that the more reliable and prolific method for synthesizing $BaTiO_3$ 1D nanostructures in ambient atmosphere is to use rod-shaped titania as the anisotropic media on which the barium precursors stick in the molten salt.

Molten-salt synthesis is a simple method for preparing ceramic products. Molten salt plays a critical role in the whole process as a reaction medium solvent, where reactants dissolve and precipitate inside. The surface and interface energies between the constituents and the salt shape the features of this synthesis method, resulting in a tendency to minimize the energies by forming a specific morphology.[27] The initial particle size and shape, the type and amount of salt, the precursor composition, the reaction temperature, and the dissolution rate of the constituents in the molten salt influence the morphologies and characteristics of the products.[27] This work used rod-shaped TiO_2 as the source of titanium, because of its highly anisotropic growth in molten salt,[28] to successively synthesize anisotropic $BaTiO_3$ nanostructures, such as cube-shaped and rod-shaped nanostructures, which are realized by means of the distinct dissolution rates of the selected barium precursors and the titanium precursor in the molten salt.

II. Experiments

The three-series products (BT-1, spherical $BaTiO_3$; BT-2, cube-shaped $BaTiO_3$; and BT-3, rod-shaped $BaTiO_3$) were synthesized with different barium and multishaped titanium precursors. BT-1 was synthesized using $BaCO_3$ as the barium precursors reacted with the spherical TiO_2 in the eutectic mixture of NaCl-KCl flux. BT-2 and BT-3 were synthesized using BaO and $BaCO_3$ ($BaCO_3$ will transform into BaO when heating over about 1450 °C that is much higher than the reaction temperature we used.) as the barium precursors reacted with the rod-shaped TiO_2 in the eutectic mixture of NaCl-KCl flux, respectively. The reagents we used were BaO, $BaCO_3$, TiO_2, KCO_3, NaCl, and KCl, which were of A. R. grade without further purification. The rod-shaped TiO_2 was synthesized and derived from rod-shaped $K_2Ti_4O_9$ washed with hot HCl. The mixture of K_2CO_3 and TiO_2 in the molar ratio of 1:3 was heated at 1000 °C for 18 h in the combustion boat (Al_2O_3 boat). Then, the as-synthesized product was washed with hot deionized water several times to remove the K_2CO_3 phase entirely and finally dried at 60 °C overnight. The product in the meanwhile was rod-shaped $K_2Ti_4O_9$ and verified by field emission scanning electron microscopy (FE-SEM, HITACHI S-4000) and powder X-ray diffraction (XRD, MAC Science, MXP18) equipped with Cu Kα radiation shown in Figures 1 (b) and (d). The rod-shaped TiO_2 was obtained by washing the rod-shaped $K_2Ti_4O_9$ powder with hot 1 M HCl solution for 2 h to get rid of K_2O phase and then heating the residue phase, $TiO_2 \cdot nH_2O$, at 700 °C for 1 h for transforming into the rod-shaped TiO_2. The scanning electron microscopy (SEM) image and powder X-ray diffraction (XRD) pattern were shown in Figures 1 (c) and (d).

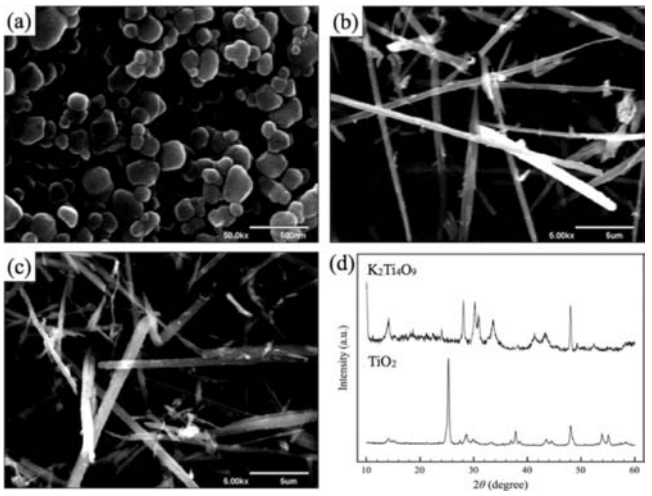

Figure 1. SEM images and powder XRD patterns of the titanium precursors: (a) SEM image of the spherical TiO_2, (b) SEM image of the rod-shaped $K_2Ti_4O_9$, (c) SEM image of the rod-shaped TiO_2 and (d) Powder XRD patterns of the rod-shaped $K_2Ti_4O_9$ and rod-shaped TiO_2.

The following details are the synthetic procedure for synthesizing BT-1, BT-2, and BT-3. For starters, the mixture of the barium and titanium precursor in the molar ratio of 1:1 was wet-mixed in the ethanol solution at 50 °C for 1 h with magnetic stirring and then dried at 50 °C for 6 h. Second, the mixture was mixed with NaCl-KCl flux (50% mol NaCl and 50% mol KCl, m.p.: 657 °C), acting as a reaction medium, in the weight ratio of 1:1 by hand-grinding in a mortar and pestle for 0.5 h. Third, the as-synthesized mixture was placed into the combustion boat and heated at 700 °C for 1 h in the furnace. The increasing rate was 5 °C/min and the product was taken out of the furnace for cooling naturally after reaction. Finally, the as-synthesized product was washed with hot deionized water several times until no chloride ions were detected by silver nitrate solution to ensure that the residue of salt was removed exhaustively and then dried at 120 °C overnight.

The as-synthesized three-series products were characterized by FE-SEM, transmission electron microscopy (TEM, Philips TECNAI 20), and powder XRD measurement. The morphology and compositions were investigated using FE-SEM and TEM equipped with an energy-dispersive X-ray spectrometer (EDS). Phase analyses were examined using powder XRD at room temperature equipped with Cu Kα radiation.

III. Results and Discussion

In the three-series products, this investigation used BaO and $BaCO_3$ as the barium precursors and TiO_2, with various

(17) Urban, J. J.; Yun, W. S.; Gu, Q.; Park, H. *J. Am. Chem. Soc.* **2002**, *124*, 1186.
(18) Joshi, U. A.; Lee, J. S. *Small* **2005**, *1*, 1172.
(19) Kang, S. O.; Park, B. H.; Kim, Y. I. *Cryst. Growth Des.* **2008**, *8*, 3180.
(20) Jiang, C. L.; Kiyofumi, K.; Wang, Y. F.; Koumoto, K. *Cryst. Growth Des.* **2007**, *7*, 2713.
(21) Chen, Y. Y.; Yu, B. Y.; Wang, J. H.; Cochran, R. E.; Shyue, J. J. *Inorg. Chem.* **2009**, *48*, 681.
(22) Hernandez, B. A.; Chang, K. S.; Fisher, E. R.; Dorhout, P. K. *Chem. Mater.* **2002**, *14*, 480.
(23) Hayashi, Y.; Kimura, T.; Yamaguchi, T. *J. Mater. Sci.* **1986**, *21*, 757.
(24) Mao, Y. B.; Banerjee, S.; Wong, S. S. *J. Am. Chem. Soc.* **2003**, *125*, 15718.
(25) Deng, H.; Qiu, Y. C.; Yang, S. H. *J. Mater. Chem.* **2009**, *19*, 976.
(26) Xia, Y. N.; Yang, P. D.; Sun, Y. G.; Wu, Y. Y.; Mayers, B.; Gates, B.; Yin, Y. D.; Kim, F.; Yan, Y. Q. *Adv. Mater.* **2003**, *15*, 353.
(27) Yoon, K. H.; Cho, Y. S.; Kang, D. H. *J. Mater. Sci.* **1998**, *33*, 2977.
(28) Kimura, T.; Yamaguchi, T. *Ceram. Int.* **1983**, *9*, 13.

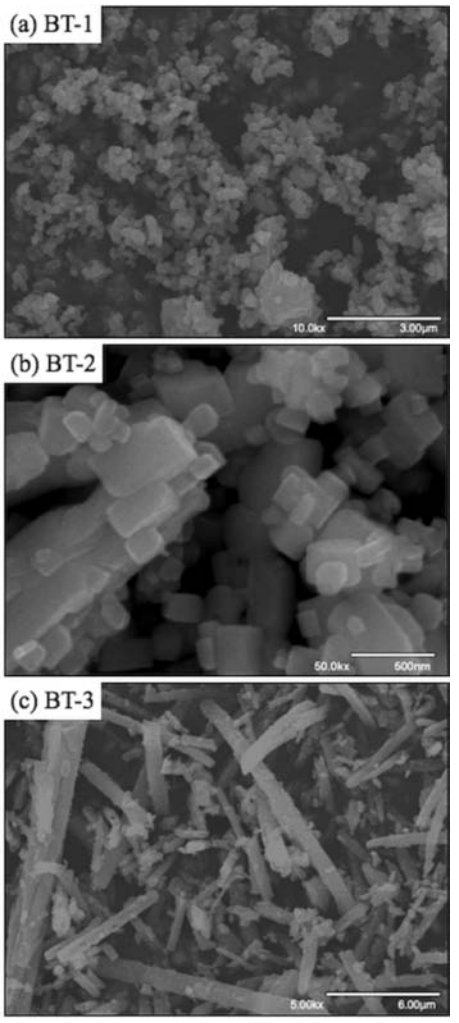

Figure 2. SEM images of the three-series products: (a) BT-1, (b) BT-2, and (c) BT-3.

morphologies, as the titanium precursors. The reaction time and temperature, 1 h and 700 °C, were the same in all the three-series synthesis processes. The SEM images shown in Figures 1 and 2 demonstrate that the shape of the products is extremely relevant to that of the titanium precursors and the dissolution rates of the barium and titanium precursors. The XRD patterns shown in Figure 3 verify there are no detectable impurity peaks in the three-series products, and the structure of the three-series products is a tetragonal structure based on the results of Rietveld refinement. The high-resolution transmission electron microscope (HRTEM) image and the selected-area electron diffraction (SAED) pattern shown in Figure 4 reveal that BT-3 was grown along the [001] direction, and the lattice fringe shows the lattice constant *a* is about 4.01 Å.

Both the BT-1 and BT-3 processes used $BaCO_3$ as the barium precursor and the spherical TiO_2 and rod-shaped TiO_2 as the titanium precursors, respectively. According to the SEM images, the products have the same shapes as the titanias used: The spherical TiO_2 resulted in spherical $BaTiO_3$; the rod-shaped TiO_2 resulted in rod-shaped $BaTiO_3$. Hence, we can effectively change the shape of the products by changing the shape of the precursors.

As a great finding, we used BaO instead of $BaCO_3$ as the barium precursor to react with the rod-shaped TiO_2 in the

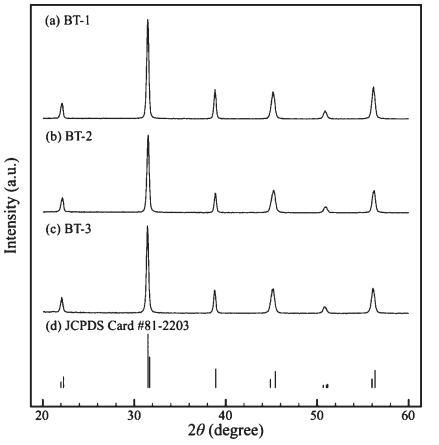

Figure 3. Powder XRD patterns of the three-series products and JCPDS Card: (a) BT-1, (b) BT-2, (c) BT-3, and (d) JCPDS Card #81−2203.

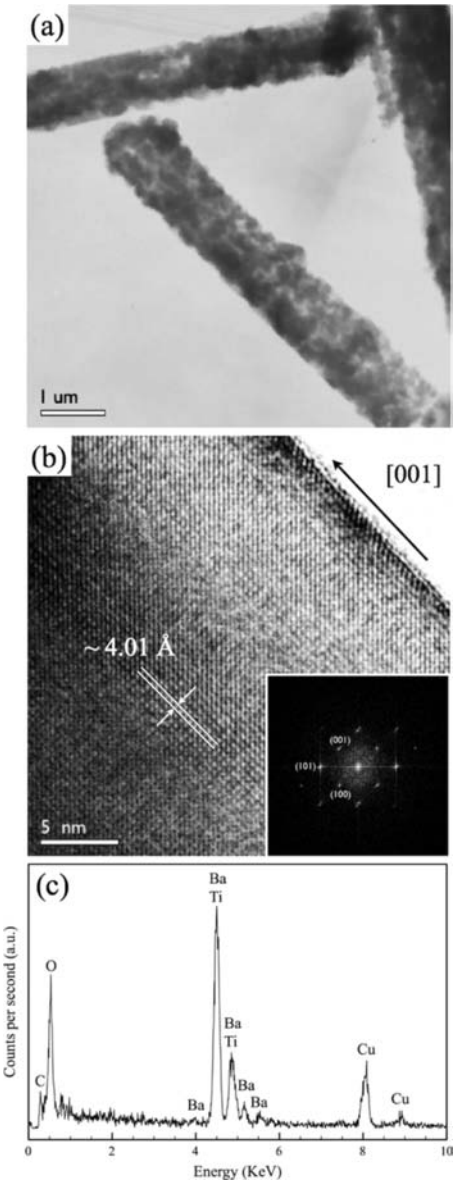

Figure 4. TEM image, HRTEM image with SAED pattern, and EDS spectrum of BT-3: (a) TEM image, (b) HRTEM image with SAED pattern and (c) EDS spectrum.

Table 1. Results of Rietveld Analysis of the Powder XRD Patterns of BT-1, BT-2, and BT-3

	JCPDS (#81−2203)	BT-1	BT-2	BT-3
$a(b)$ (Å)	3.990	3.9954(5)	4.0002(6)	4.0099(6)
c (Å)	4.035	4.0140(8)	4.0211(2)	4.0253(2)
c/a	1.011(3)	1.0046(6)	1.0052(1)	1.0038(3)
Vol. (Å^3)	64.237(6)	64.0776(4)	64.3462(8)	64.7262(6)
Z(Ti)	NA	0.4685(6)	0.4984(8)	0.4837(8)
Z(O1)	NA	1.0001(4)	0.9796(7)	0.9968(4)
Z(O2)	NA	0.5090(4)	0.4983(4)	0.4909(0)
R_{wp} (%)	NA	10.47	10.17	10.47

molten salt. This yielded BT-2 in contradistinction to BT-3. Because of the "break-up" of the rod-shaped TiO_2 when heated individually in NaCl-KCl flux at 700 °C for 1 h and the unchangeableness of BT-3 when heated for another 1 h at 700 °C in NaCl-KCl, the shape changes from a rod-shape to a cube-shape in BT-2 might be ascribed to the "break-up" of the rod-shaped TiO_2 before or during the reaction.

The lattice constants a and c of BT-1, BT-2, and BT-3 were calculated using Rietveld refinement and tabulated in Table 1. Figure 5 shows the results of Rietveld refinement with the difference curves below each Rietveld analysis. The tetragonalities (c/a ratio) of BT-1, BT-2, and BT-3 are 1.0046(6), 1.0052(1), and 1.0038(3), respectively. All are larger than 1, which means the unit cells of the three-series products are all in tetragonal structure, attributed to surface relaxation.[29] Since particle sizes in the a-direction of BT-1, BT-2, and BT-3 are all at the nanoscale and smaller than that of bulk, they experience surface relaxation and thus increase the $a(b)$ values for minimizing free energy. On the other hand, because particle sizes in the c-direction of both BT-1 and BT-2 are at the nanoscale and of BT-3 is at the microscale similar to the scale of microparticles (bulk), the behavior of BT-3 in the c-direction is much like that of bulk. Thus, the c value of BT-3 is closer to that of bulk, which is 4.035 Å, and larger than that of BT-1 and BT-2. Consequently, because all three-series products have larger a values and smaller c values than bulk, the c/a ratios of BT-1, BT-2, and BT-3 are smaller than that of bulk.

This work also used a two-peak fit method to decompose the overlapping (002) and (200) diffraction peaks (see Figure 6). The lattice constant a and c of the three-series products can be calculated using Bragg's law, and the results are similar to the results derived from Rietveld refinements. As a result of the isotropic particle structure of BT-1 and BT-2, BT-1 and BT-2 arrange randomly without dominant orientation on the substrate. Thus, the intensity ratio between the (200) and (002) diffraction peaks is close to 1:2 because the (200) and (020) peaks are inseparable (see Figures 6 (a) and (b)). On the contrary, because BT-3 has an anisotropic particle structure, the c-direction axis lies on the substrate with higher probability than standing erectly on the substrate. Therefore, the intensity of the (200) peak is much higher than that of the (002) peak in XRD measurement (see Figure 6 (c)).

On the basis of the above observations, the dissolution rate of the reactants in the molten salt plays an important role that critically affects reaction rate and morphology of the products in the synthesis. On the one hand, if both reactants are soluble in the molten salt, the dissolution−precipitation mechanism may be the dominant mechanism throughout the synthesis; the

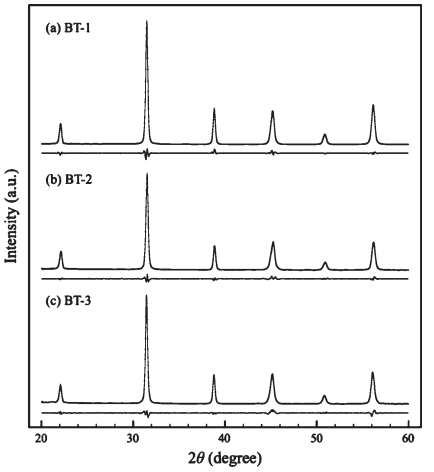

Figure 5. Rietveld refinements of the powder XRD patterns of the three-series products: (a) BT-1, (b) BT-2, and (c) BT-3. The difference curves are displayed below each Rietveld analysis and have been offset for clarity.

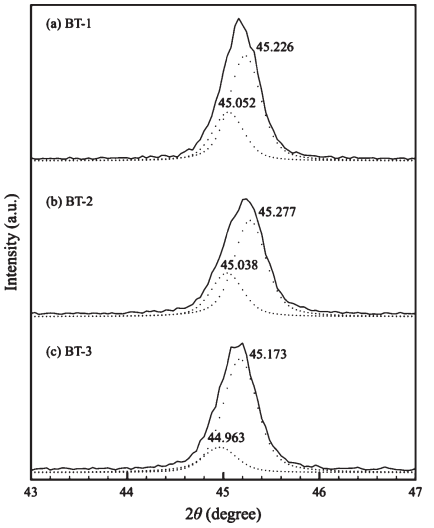

Figure 6. Two-peak fit of the powder XRD patterns at (200) and (002) peaks of the three-series products: (a) BT-1, (b) BT-2, and (c) BT-3.

product will readily synthesize via precipitation from the salt containing the dissolved reactants.[30,31] On the other hand, if one reactant is much more soluble than the other, an *in situ* transformation mechanism will be the dominant mechanism in the synthesis; the more soluble one will dissolve into the salt at an early reaction stage, then diffuse onto the surfaces of the less soluble reactant, and finally react to form the product.[31] According to this argument, this work infers that the dissolution rate in the molten salt of $BaCO_3$ used in BT-3 is faster than that of BaO used in BT-2 because the rod-shaped TiO_2 preserves the initial morphology in BT-3 instead of breaking up into several cube-shaped TiO_2 in BT-2.

Figure 7 shows the proposed synthetic diagrams as a more precise synthesis of the $BaTiO_3$ synthetic mechanism in the molten salt. The following details are the main steps: The mixture of $BaCO_3$, TiO_2, and NaCl-KCl flux was put in

(29) Ishikawa, K.; Uemori, T. *Phys. Rev. B* **1999**, *60*, 11841.

(30) Eckert, J. O.; HungHouston, C. C.; Gersten, B. L.; Lencka, M. M.; Riman, R. E. *J. Am. Ceram. Soc.* **1996**, *79*, 2929.

(31) Byrappa K.; Ohachi T. *Crystal Growth Technlogy*; Springer: New York, 2002.

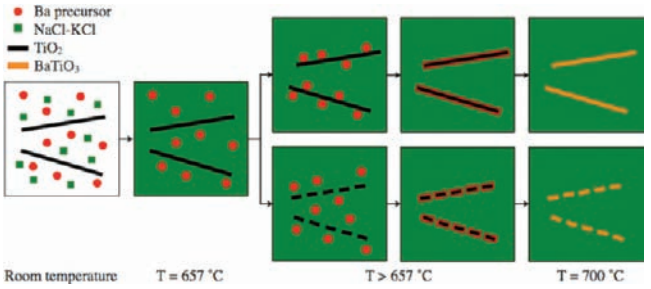

Figure 7. Proposed schematic diagram of the synthetic mechanism of $BaTiO_3$ in the molten salt: the upper flow is due to the faster dissolution rate of the barium precursor than that of the titanium precursor, and the lower flow is due to the slower dissolution rate of the barium precursor than that of the titanium precursor.

the combustion boat at room temperature. By increasing the temperature at a constant rate to the melting point of NaCl-KCl flux (ca. 657 °C), NaCl-KCl flux transformed into molten salt, acting as a solvent where $BaCO_3$ and TiO_2 acted as solutes and dissolved inside. In the first flow of the proposed schematic diagram (the dissolution rate of the barium precursor is faster than that of the titanium precursor), because of faster dissolution rate of $BaCO_3$ compared to TiO_2, $BaCO_3$ dissociated and dissolved into the molten salt primarily upon further heating, then readily dispersed to the periphery of TiO_2, covering the entire surface of TiO_2 to form the BT-shell, which hindered the rod-shaped TiO_2 from the break-up process. Finally, after $BaCO_3$ diffused through the BT-shell and reacted with TiO_2 completely, this work obtained the rod-shaped $BaTiO_3$ having the same morphology as the TiO_2 precursor used.

In the second flow of the proposed schematic diagram (the dissolution rate of the barium precursor is slower than that of the titanium precursor), the mixture of BaO, TiO_2, and NaCl-KCl flux experienced processes similar to the first flow before NaCl-KCl flux transformed into the molten salt. Because of slower dissolution rate of BaO compared to $BaCO_3$, the rod shaped TiO_2 had the chance to break up into several fragments from the grain boundaries in the molten salt before BaO dissociated and dissolved into the molten salt, forming a BT-shell outside the surface of the rod-shaped TiO_2. As a result of the break-up process of the rod-shaped TiO_2 before BT-shell formation, this work finally derived the cube-shaped $BaTiO_3$ having high quality without impurity peaks in the XRD pattern.

IV. Conclusion

This study reports the development of a simple synthetic process for synthesizing morphology-controlled $BaTiO_3$ nanostructures such as spherical, cube-shaped, and rod-shaped $BaTiO_3$. Findings show that the initial shape of the titanium precursors can critically determine the shape of the final products. Further findings show that the dissolution rates of the barium and titanium precursors play important roles in molten-salt synthesis. We obtained the spherical $BaTiO_3$ using the spherical TiO_2 as the titanium precursor and obtained the rod-shaped $BaTiO_3$ using the rod-shaped TiO_2 as the titanium precursor. However, when we used another barium precursor, BaO, with slower dissolution rate, the rod-shaped TiO_2 broke up into several cube-shaped TiO_2 before reacting with BaO, because of failure of forming the BT-shell to hinder the break-up process of the rod-shaped TiO_2. Therefore, we finally obtained the cube-shaped $BaTiO_3$. The powder XRD patterns show good quality and crystallinity of the $BaTiO_3$ nanostructures, and the SEM images show that the morphologies of the final product all match very consistently with the titanium precursors.

Acknowledgment. This work is partially supported by the National Science Council of Taiwan under grant NSC-96-2628-M-009-001-MY3 and NSC-95-2221-E-133-001.